Effect of Ca addition on the oxidation resistance of Ni-Al alloy

Chihiro Tabata[1,2,3,*], Kyoko Kawagishi[1,3], Tadaharu Yokokawa[1], Jun Uzuhashi[1], Tadakatsu Ohkubo[1], Hiroshi Harada[1,4] and Shinsuke Suzuki[2,3,5]

1. National Institute for Materials Science (NIMS), 1-2-1 Sengen, Tsukuba, Ibaraki 305-0047, Japan
2. Department of Applied Mechanics and Aerospace Engineering, Waseda University, 3-4-1 Okubo, Shinjuku-ku, Tokyo 169-8555, Japan
3. Department of Materials Science, Waseda University,3-4-1 Okubo, Shinjuku-ku, Tokyo 169-8555, Japan
4. (Present address) Superalloy Design Laboratory, 3-18-33, Azuma, Tsukuba, Ibaraki, 305-0031, Japan
5. Kagami Memorial Institute for Materials Science and Technology, Waseda University, Tokyo 169-0051, Japan

*Corresponding author
chihiro448@akane.waseda.jp (C. Tabata)

Abstract:

Ni-base superalloys are known for their high temperature oxidation resistance, however, impurity of S at ppm order can significantly decrease the oxidation resistance of the alloy. Melting using a CaO crucible is reported to improve the oxidation resistance, but Ca can negatively impact the oxidation resistance of the alloys, depending on the amount and method of addition. The objective of this research was to determine the effect of Ca addition using Al-Ca alloy, and to understand how Ca affects the oxidation resistance of the alloy. Single crystal Ni-9.8 wt.% Al model alloys melted in an Al_2O_3 crucible were cast, with the addition of 20 ppm of S in all samples, and 0, 20, and 100 ppm of Ca using Al-4.9wt.%Ca alloy. Ca addition improves the oxidation resistance of the samples, though it lacked in efficiency in the improvement of this trait compared to when using a CaO crucible. Increasing the amount of Ca addition led to the increase in the amount of CaS formation and desulfurization, though the removal of slag is crucial. Although Ca was effective in terms of desulfurization, to limit the negative effects of Ca itself, the formation of sulfides must be the dominating reaction.

(max 200 words)

Keyword: oxidation, sulfur segregation, Ca addition, CaS, single crystal superalloy

I. Introduction

Ni-base superalloys are widely used in jet engines and other gas turbine systems, due to their excellent mechanical properties and oxidation resistance [1]. Recent heightened awareness of establishing a sustainable society requires the alloys with higher temperature capability to reduce CO_2 emissions and increase the thermal efficiency of turbines. For this reason, many rare metals are used in the alloys to improve their mechanical properties. But due to the recent increase in the price of the rare metals, ways to recycle and reuse materials are strongly required. Used turbine blades contain large amounts of S contamination, which often comes from the fuels, inlet air, and the materials used to cast the alloys. This degrades their properties, especially oxidation resistance, in high temperature environment [2]. S is known to segregate at the oxide and substrate interface, decreasing the adhesion of oxides, resulting in the spalling of oxides [3-7]. Even S at ppm level can have a detrimental effect on the alloy, therefore, ways to remove and prevent the segregation of S are necessary [8,9].

One way to desulfurize the alloys is to use CaO. Harada *et al.* and Utada *et al.* developed a method using CaO crucible to melt turbine components made of Ni-base superalloys, removing impurities such as S before casting [10,11]. Utada *et al.* proved that this method desulfurized the Ni-base superalloy samples and improved the oxidation resistance, all the while maintaining its mechanical properties [12]. Sugiyama *et al.* also used this method and found that the samples melted in a CaO crucible had higher oxidation resistance compared to the ones melted in an Al_2O_3 crucible, even though the S content of the two samples were about the same [13]. According to previous research, it was revealed that the S segregation for the sample melted in CaO crucible was lower than the one melted in Al_2O_3 crucible [14]. Researches indicate that the CaO reacted with the Al within the melt, forming calcium aluminates and Ca, and the excess Ca reacted with S to form CaS, preventing S from segregating to the interface of the Al_2O_3 oxide layer and the Ni-base substrate [12,14,15]. In order to simplify the reaction, similar tests were conducted for Ni-Al binary alloys. The usage of CaO crucible on Ni-Al alloy also proved to be effective, and the mechanism and location for the formation of CaS has been clarified [16]. According to Yokokawa *et al.*, CaO pellets were also effective in the removal of S from the melt [17]. On the other hand, CaO is known to easily hydrate, making it difficult to use CaO crucibles at an industrial level [18,19]. Therefore, ways to improve this method are needed.

Although CaO improved the oxidation resistance of the alloys, excessive Ca addition and CaO deposits from the different types of coals and geographic locations the turbines were used in, are known to degrade the oxidation resistance of the superalloys. Azakli *et al.* reported that excessive amounts of Ca decreased the oxidation resistance of the alloys, due to the formation of Ca-rich complex oxides [20]. DeBarbadillo also found that excess Ca can form intermetallic compounds with Ni that are brittle and moisture-sensitive, which resulted in severe hot tearing of the Ni-base alloy [21]. Reports on CaO deposits showed an increase in the oxidation rate and degradation rate of the samples [22,23]. Jung *et al.* also observed significant degradation during cyclic oxidation at 950°C for both coated and uncoated superalloys by CaO deposits [24]. Yet, the difference in the mechanism behind the usage of CaO and the Ca addition is not clear. Also, in contrast with the effect of mass addition of Ca as described above,

the effect of limited addition of Ca on the oxidation resistance of the alloys has not been investigated.

The objective of this research is to determine whether it is possible to desulfurize the alloys by the addition of Ca at ppm level using Al-Ca alloy, and to understand how Ca affects the oxidation resistance of the Ni-Al binary single crystal alloy. In order to simplify the reactions between the melt and the crucible, and to compare the results with our previous research, Ni-Al binary single crystal alloys were used for this research. The oxidation resistance of the samples at 1100°C were investigated, and the reaction between the melt and the crucible were observed.

II. Experimental Procedures

Ni-9.8 wt.% Al alloys were melted in an Al_2O_3 crucible at 1600 °C with the pressure kept under 6×10^{-2} Pa, using a directional solidification furnace with high frequency vacuum induction heating. S was added using NiS powder that was inserted within a Ni tube, and Ca was added using Al-4.9 wt.% Ca alloy. 20 ppm of S was added in all 3 samples, and 0, 20, and 100 ppm of Ca were also added to each sample, which will be referred to as Ni-Al (0 ppm Ca), Ni-Al (20 ppm Ca), and Ni-Al (100 ppm Ca). After the addition of S and Ca, the melt was kept for 15 min and was poured from the crucible into a ZrO_2-base mold kept at 1500 °C, and unidirectionally solidified into single crystal round bars of 11 mm in diameter and 135 mm in length. The mold was withdrawn from the heating chamber to the cooling chamber at 200 mm/h. “Starters” are placed at the bottom of the mold, which solidifies the melt into columnar grained, polycrystalline alloys. The “selectors” exist between the starters and the cylindrical sample to help solidify the melt into a single crystal alloy. Solution-heat-treatment was performed at 1300 °C for 5 h, and aging heat-treatment was performed at 870 °C for 20 h in vacuum using a high frequency induction heat treatment furnace [10].

The chemical composition was analyzed using the same methods as our previous research [16]. For Ni and Al, an inductivity coupled plasma optical emission spectrometer (ICP-OES, Aligent, ICP-OES 720-ES) was used, while glow discharge mass spectrometry (GD-MS, Nu Instruments LTC. ASTRUM) was used for S and Ca. Oxidation testing samples were also prepared following the same procedures as our previous research [16], where the samples were cut from the cylinders to be 5 mm in height and 9 mm in diameter, with the surfaces finished using U.S. Grid #600 SiC abrasive paper.

The remaining Ni-Al alloy on the bottom sides of Al_2O_3 crucibles after pouring were analyzed in order to understand what kinds of reactions occurred during the melting process. The samples were embedded in resin and observed using electron probe micro analyzer with a field emission electron gun (FE-EPMA, SHIMADZU, EPMA-8050G). Inclusions found within the starters were observed using scanning electron microscopy (SEM) with energy dispersive X-ray spectroscopy (EDS) (ZEISS, GeminiSEM300). Cyclic oxidation tests were performed at 1100°C for 100 cycles, with each cycle containing 1 h of heating in air and 1 h of cooling in air, and the samples were weighed after several cycles. Samples oxidized at 1100°C for 1 h were also prepared, and the oxide scales were observed using SEM (CrossBeam 550, ZEISS) and aberration corrected scanning transmission electron microscope (STEM, FEI Titan G2 80-200) with energy dispersive X-ray spectroscopy (EDS) at the

acceleration voltage of 200 kV. The inclusion found within the sample were also lifted out and prepared using focused ion beam (FIB)-SEM dual beam system (FEI Helios G4UX). High-angle annular dark field (HAADF)-STEM images and EDS elemental maps were taken by STEM, also selected area electron diffraction (SAED) images were taken from TEM mode of STEM.

III. Results

Fig. 1 shows the backscattered electron image and elemental maps taken using FE-EPMA for Ni-Al (20 ppm Ca), close to the bottom side of the Al_2O_3 crucible. Areas that appeared black in the BSE images were observed. According to the EPMA mapping and line scan results, Al and O were detected in similar locations, which are most likely Al_2O_3. Ca was also observed in some of the same parts as Al and O, indicating that Ca-Al-O slags were observed inside of the Ni-Al melt. S was detected both within and around the slag, resulting in the removal of S from the alloy. Although several regions of the alloy had S signal without associated Ca signal, it is uncertain whether aluminum sulfides had formed or if Ca had existed previously. **Fig. 2** also shows the backscattered electron image and elemental maps taken using FE-EPMA, this time for Ni-Al (100 ppm Ca). Compared to **Fig. 1**, large amount of Ca was observed in the same place as Al and O. S was also detected, but more frequently and at a larger amount. This indicates that increasing the Ca content resulted in the increase in the amount of desulfurization.

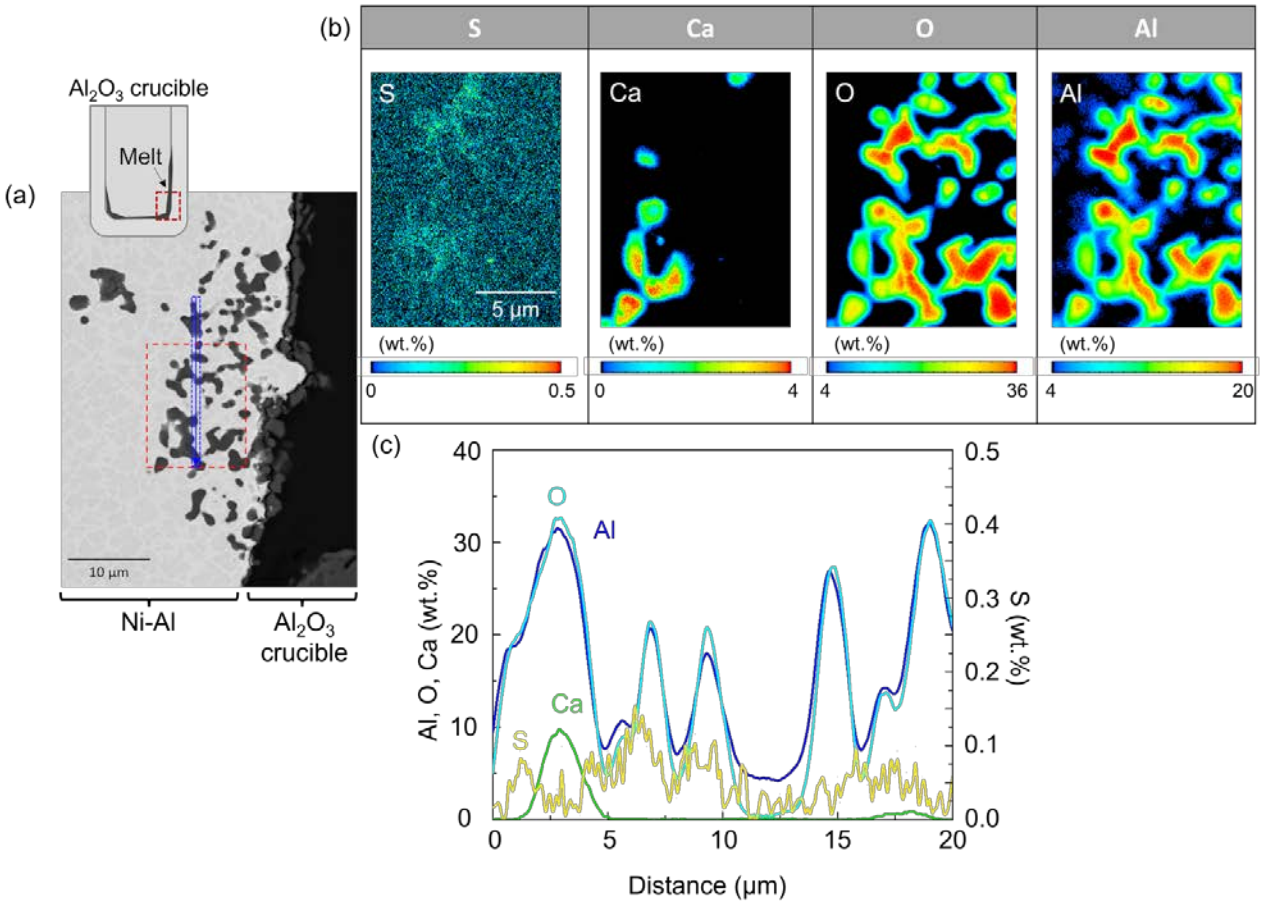

Fig. 1 (a) Backscattered electron image and (b) FE-EPMA elemental maps for S, Ca, O, and Al taken from the remaining Ni-Al (20 ppm S, Ca) near the bottom of the Al_2O_3 crucible used to melt the sample. The red rectangle in the backscattered electron image (a) indicates where the elemental maps were taken. (c) Line profiles were taken for S, Ca, O, and Al, from the area shown in blue.

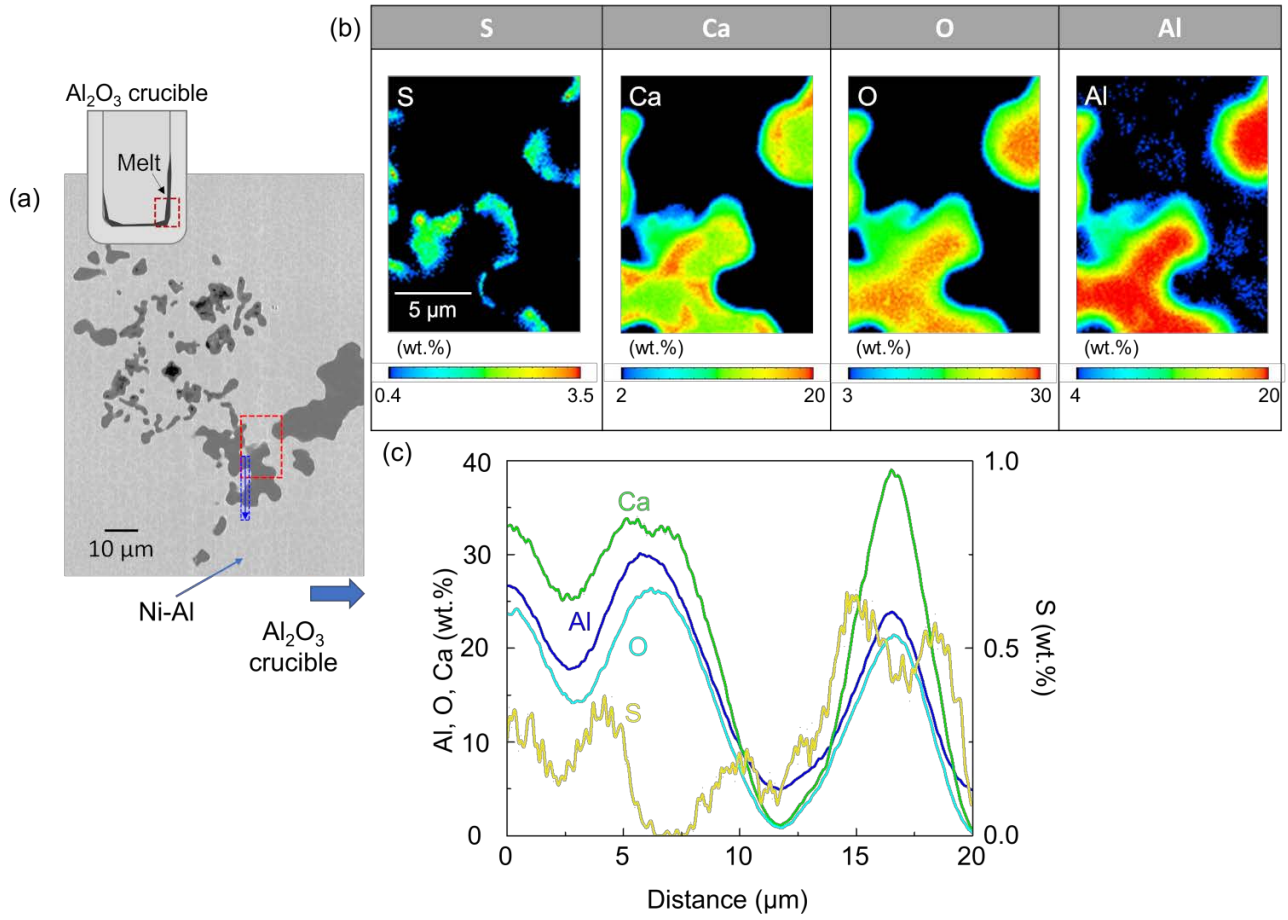

Fig. 2 (a) Backscattered electron image and (b) FE-EPMA elemental maps for S, Ca, O, and Al taken from the remaining Ni-Al (100 ppm Ca) near the bottom of the Al_2O_3 crucible used to melt the sample. The red rectangle in the backscattered electron image indicates where the elemental maps were taken. (c) Line profiles were taken for S, Ca, O, and Al, from the area shown in blue.

In order to understand whether Ca addition could form CaS inclusions to suppress S segregation at the interface between Al_2O_3 oxide layer and the substrate, as when using a CaO crucible, the starters were observed using SEM-EDS in **fig. 3** and **fig. 4.** What appears to be inclusions formed within the voids, or inclusions promoting the formation of voids were found near the grain boundary and the eutectic γ′ phase, most likely in the inter-dendritic regions, for both Ni-Al (20 ppm Ca) and Ni-Al (100 ppm Ca) samples. The peaks of Ca and S were observed, indicating that CaS had formed, similar to the results for melting using a CaO crucible [16]. For each sample, the width and the height of 10 inclusions were measured, and the average size of the inclusions were calculated. For

Ni-Al (20ppm Ca), the inclusions were 379 nm in width and 338 nm in height average. For Ni-Al (100 ppm Ca), the inclusions were 747 nm in width and 726 nm in height. The number of inclusions found within an area of a certain size have not changed drastically. These results indicate that the increase in the Ca content led to the increase in the size of the inclusions.

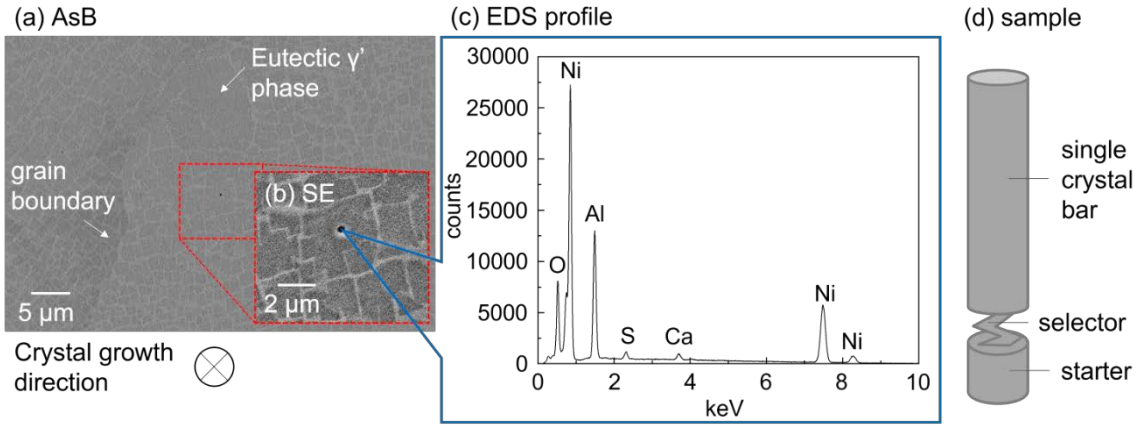

Fig. 3 (a) Angle selective BSE image and (b) SE image of the as-cast starter of Ni-Al (20 ppm Ca), (c) the peak profile of the inclusion, taken using EDS, and (d) schematic diagram of the cast sample to show the starter.

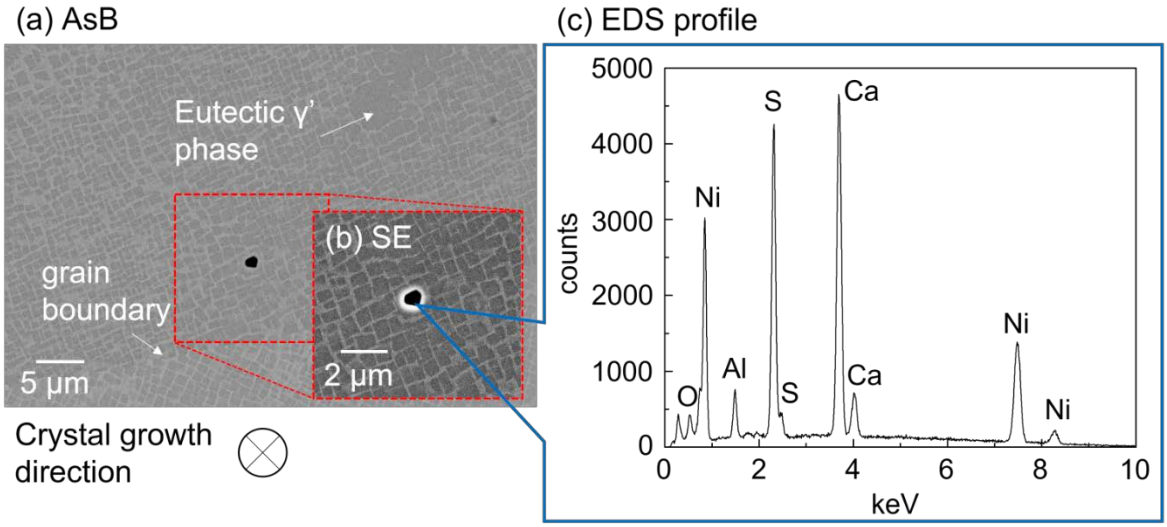

Fig. 4 (a) Angle selective BSE image and (b) SE image of the as-cast starter of Ni-Al (100 ppm Ca) and (c) the peak profile of the inclusion, taken using EDS.

In order to determine whether the inclusions were actually CaS, the inclusion found within the starter of Ni-Al (100 ppm Ca) was lifted out using FIB-SEM system and observed by STEM. **Fig. 5(a)** shows the cross sectional HAADF-STEM image and the EDS elemental maps of the inclusion. Ca-S inclusion of about 300 nm in size was detected, with a formation of a void above. SAED

pattern was also taken from the inclusion and shown in **Fig. 5(b)**. Judging from the SAED patterns and the crystal orientations of the substrate fcc-Ni_3Al, mismatched fcc-CaS crystals have formed, similar to the ones detected when using a CaO crucible [16]. The inclusions likely form either at the voids or promote the formation of voids.

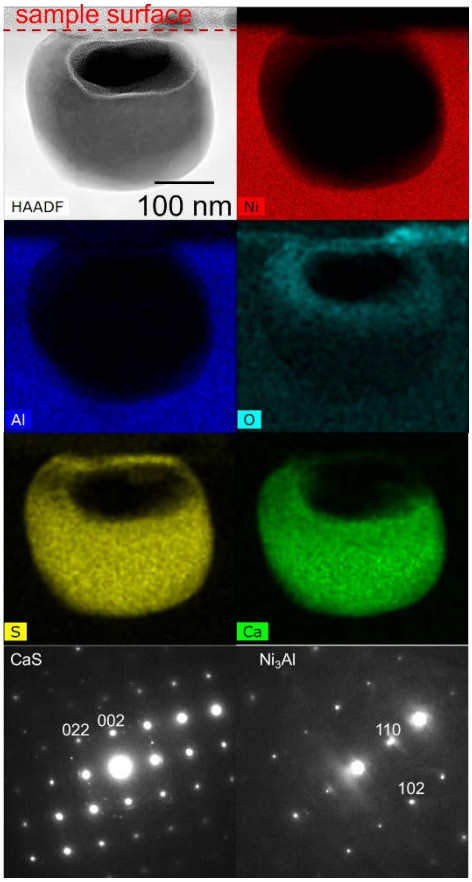

Fig. 5 (a) Cross sectional HAADF-STEM image and EDS elemental maps of the inclusion found within the starter of Ni-Al (100 ppm Ca). (b) Selected area electron diffraction (SAED) pattern taken from the inclusion presented in (a). The electron beam was incident along the [110] direction for CaS, and $[2\bar{2}\bar{1}]$ direction for Ni-Al.

To determine whether Ca addition had any effect on the oxidation resistance of the samples, cyclic oxidation tests were conducted at 1100 °C. **Fig. 6** shows the cyclic oxidation results of Ni-Al (0 ppm Ca) and Ni-Al (20 ppm Ca). Note that Ni-Al (100 ppm Ca) was removed from the results, and the reason for this will be explained in the discussion section. Results for Ni-Al without any S additions, taken in our previous research, are also included as a reference [16]. Ca addition did result in the increase of oxidation resistance, compared to the sample with the addition of S only. However, it did not have as much effect on the cyclic oxidation resistance as the sample melted using a CaO crucible. **Table I** shows the results of the chemical composition of both the 20 ppm Ca added sample and the non-Ca added sample, both of which are done before the oxidation tests, using ICP-OES for Al and

GD-MS for S and Ca. The results indicate that the improvement in the cyclic oxidation was due to both the decrease in the S content with the addition of Ca, and the suppression of the oxide spallation by the formation of CaS. However, most of the Ca has not been detected within the sample and its content was significantly lower than intended, since most of the Ca added had reacted with the Al_2O_3 crucible and did not remain within the alloy. There was also an increase in the Al content for both samples, which likely came from the Al_2O_3 crucible. The Al_2O_3 crucible itself does not have the ability to remove S from the alloy, therefore, the decrease in the S content is due to the addition of Ca. The reaction between the Al_2O_3 crucible and the added Ca likely led to the formation of the calcium aluminates slag, which is known to remove S from the alloy [12-16]. Although there is the possibility of the formation of CaS directly after the addition, we believe most of the added Ca will likely react with the Al_2O_3 crucible first, before forming CaS within the melt. This is likely due to the order of the reactions that had occurred. As it will be shown in the discussion section by the Gibbs free energy calculations, when S and Ca are added within the melt, oxides will form before the sulfides. The decrease in the S content is most likely due to this reaction, leading to the increase in the oxidation resistance observed in the cyclic oxidation test result in **Fig. 6**.

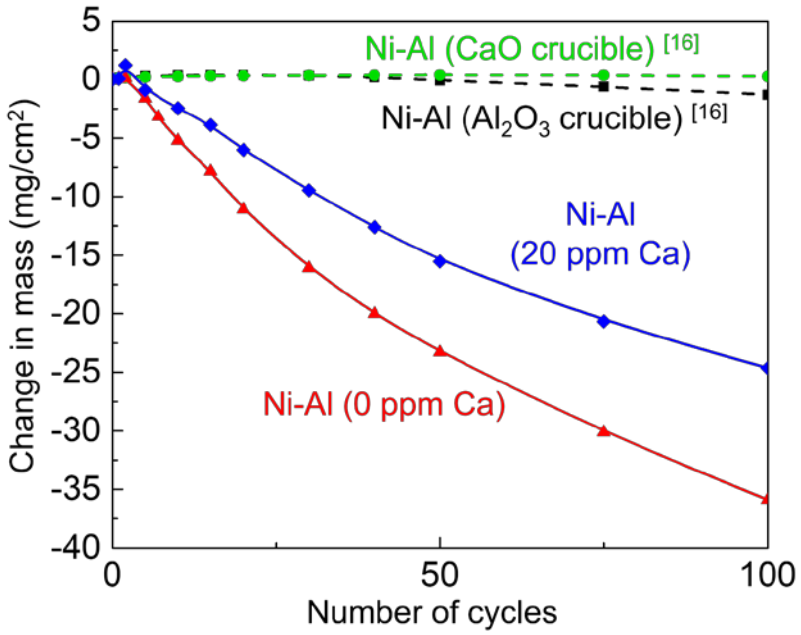

Fig. 6 Cyclic oxidation results for Ni-Al (0 ppm Ca) and Ni-Al (20 ppm Ca) at 1100 °C for 100 cycles. Results for Ni-Al melted in an Al_2O_3 crucible and a CaO crucible are also included as a reference [16].

Table I Analyzed chemical compositions of the single crystal alloys used in this study (Ni bal.)

Sample	Al (wt.%)	S (ppm)	Ca (ppm)

Ni-Al (Al_2O_3 crucible) [16]	9.80	2	-
Ni-Al (CaO crucible) [16]	9.76	3	6
Ni- Al (0 ppm Ca)	10.0	23	-
Ni-Al (20 ppm Ca)	10.1	13	0.2

Samples of Ni-Al (0 ppm Ca) and Ni-Al (20 ppm S, Ca) that had been oxidized at 1100 °C for 1 h were lifted out using FIB, and the oxide scales were observed using in-lens secondary electron (IL-SE) SEM and STEM-EDS, as shown in **Fig. 7**. **Figure 7(a)** shows the results for Ni-Al (0 ppm Ca). Although Al rich regions were detected, the Al_2O_3 scales are not continuous, and the scale width for each layer of oxides was not even. On the other hand, the width of the oxide scales found in Ni-Al (20 ppm Ca) was even, and continuous Al_2O_3 layers had formed, as shown in **Fig. 7(b)**. Ca could not be detected for both samples. The results suggest that Ca addition led to the removal of S from the alloy, and the reduced S content led to the formation of continuous oxides. However, as it can be seen in **Table I**, amount of S removed was not enough to fully prevent the oxide spallation.

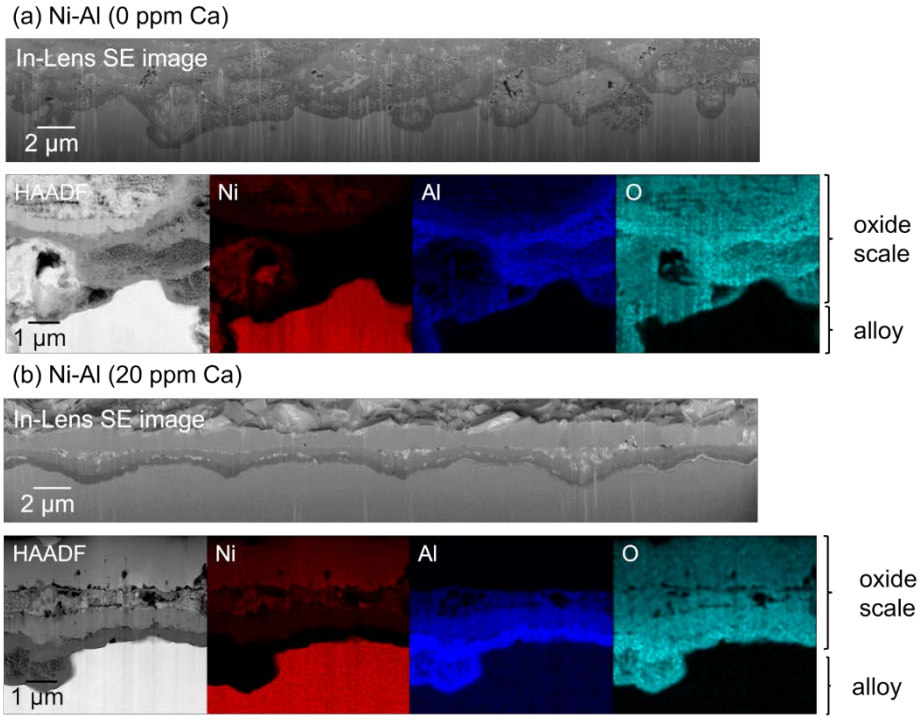

Fig. 7 In-Lens secondary electron (IL-SE) SEM images, HAADF-STEM images, and EDS elemental maps of the oxide scales of (a) Ni-Al (0 ppm Ca) and (b) Ni-Al (20 ppm Ca), which were oxidized at 1100 °C for 1 h.

IV. Discussion

Judging from the results in **Fig. 1 to Fig. 5**, larger amounts of Ca addition led to the increase in the desulfurization of the melt and formation of CaS. It can be assumed that large amount of Ca addition could lead to the increase in oxidation resistance of the sample. However, for this experiment, several inclusions, which are most likely parts of the slag formed during the reaction between the Al_2O_3 crucible and the melt, had ended up within the metal. This resulted in the formation of cracks in the starters, as shown in **fig. 8**. Presumably, part of the slag that had formed during the reaction between the Al_2O_3 crucible and added Ca had entered the melt, and this may negatively affect the oxidation resistance of Ni-Al (100 ppm Ca) sample. For this reason, the cyclic oxidation results for Ni-Al (100 ppm Ca) had been removed from **Fig. 6**. For this experiment, filters were not used when pouring the melt into the cast, in order to prevent the Ni-Al melt from clogging up the filter. Filters can most likely remove any sorts of slags that could get involved by the melt, preventing the Ca-Al-O-S slags from getting in the metal, preventing the decrease in the oxidation resistance of the sample.

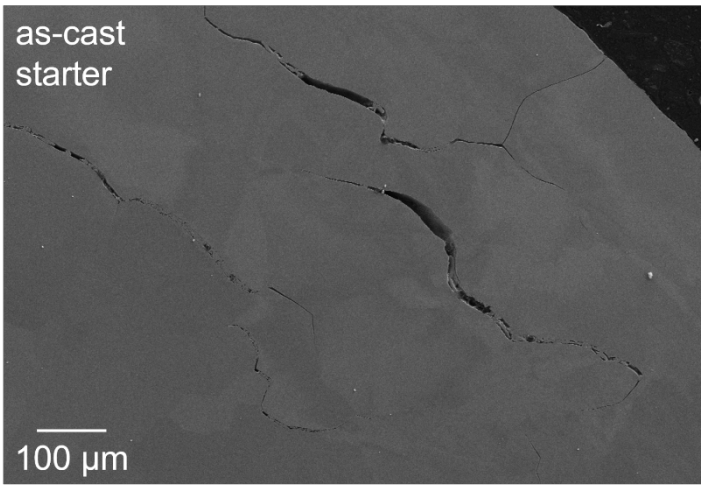

Fig. 8 SEM image of the cracks found within the as-cast starter of Ni-Al (100 ppm Ca).

Next, we will discuss the differences in the reactions for the usage of CaO crucibles for melting and Ca addition. **Figure 9** presents the schematic diagram of the reactions that had likely occurred in the two processes. When considering the efficiency of melting using a CaO crucible or Ca addition, it is crucial to consider the two kinds of reaction that had occurred. The first reaction is the desulfurization by the reaction between the melt and the crucible. The second reaction is the trapping of the S by the formation of CaS. One of the major differences between the effect of Ca from the Ca addition and the usage of CaO crucible is where Ca is located initially. For the usage of the CaO crucible (**Fig. 9 (a)**), Ca is located within the crucible. The amount of Ca within the crucible is significantly larger than the amount of S within the melt. When using a CaO crucible, large amounts of slag will form, which results in the highly efficient desulfurization of the melt. Enough Ca will continue to be supplied within the melt by the reduction process of CaO, resulting in large amounts of CaS formation. On the other hand, for Ca addition (**Fig. 9 (b)**), Ca is located within the melt, and its amount is similar to or slightly larger than S. The amount of slag that can be formed is limited,

lowering the efficiency of the desulfurization process. Because the Ca within the melt reacts with the crucible, the amount of Ca that can react with the remaining S within the melt will decrease significantly, lowering the efficiency of CaS formation. Therefore, the efficiency of melting using a CaO crucible is notably higher than Ca addition.

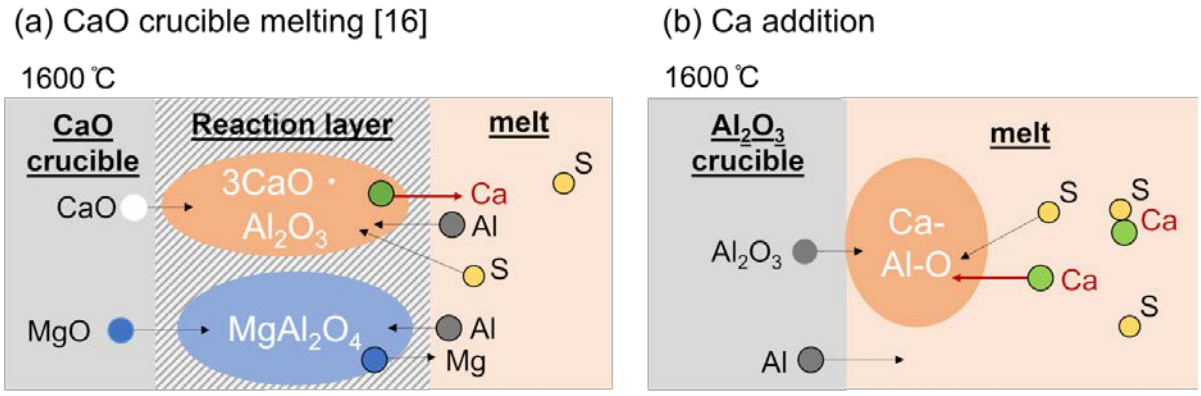

Fig. 9 Schematic diagram of the reaction between the melt and the crucible for (a) the usage of CaO crucible (adapted from [16]) and (b) addition of Ca to the melt.

Another factor that needs to be considered is the order of the reaction that had occurred. When melting using a CaO crucible, as mentioned in our previous research, the order of the reactions are as follows [12,15,16,25,26]:

$$3CaO(\text{within the crucible})+2Al(\text{within the melt})=3Ca+Al_2O_3 \quad (1)$$

$$CaO(\text{from the crucible})+Al_2O_3(\text{from previous reaction})=\text{calcium aluminates} \quad (2)$$

$$Ca(\text{from equation}(1))+S(\text{within the melt})=CaS \quad (3)$$

On the other hand, the reactions for Ca addition are most likely as follows:

$$Ca(\text{within the melt})+O(\text{within the melt or crucible})+Al_2O_3(\text{within the crucible})=\text{calcium aluminates} \quad (4)$$

$$Ca(\text{remainders within the melt})+S(\text{within the melt})=CaS \quad (5)$$

The dominant reaction of Ca was with the Al_2O_3 crucible, since Al_2O_3 crucible on its own cannot desulfurize the alloy, as it can be seen in table I, and the slight increase in the amount of Al is likely the result of this reaction. With equation (4), the Ca within the melt reacts with the crucible to form slags, which helps with the desulfurization process. But the remaining amount of Ca for equation (3) is higher than equation (5). This is because for Ca addition, the oxygen found within the melt, the crucible, or the furnace itself, reacts to form CaO or calcium aluminates before the formation of CaS. The equations below demonstrate the Gibbs free energy (J/mol) of CaO, $CaAl_2O_4$, and CaS, taken from the thermochemical database at around 1600 °C (1800K for $CaAl_2O_4$) [27-29]:

$$2\Delta G^0_{CaO} = -852 \times 10^3 \ \text{J/mol} \quad (6)$$

$$\Delta G^0_{CaAl_2O_4} = -168 \times 10^4 \ \text{J/mol} \quad (7)$$

$$2\Delta G^0_{CaS} = -684 \times 10^3 \ \text{J/mol} \quad (8)$$

The formation energy is higher for oxides than for sulfides, thus explaining how the reaction to form

CaS is inefficient, unless specific measures are taken to ensure its formation. For the usage of the CaO crucible, the reaction starts off with Ca at a stable state of CaO. The Al within the melt starts off the reduction process, creating Ca. Although some of the Ca may react with the few ppm of O within the melt, most of it will react with S. The initial structure and the reduction process likely led to the efficient formation of CaS. On the other hand, when the initial structure is Ca, as demonstrated in equations (6-8), oxides will form before sulfides. Therefore, only parts of S get desulfurized or form CaS.

Increasing the amount of Ca may help with the efficiency of the reaction, but it will also increase the formation of other oxides such as CaO or $CaAl_2O_4$. The reason other Ca addition and CaO deposits reduced the oxidation resistance for the alloys was due to the formation of these oxides [20,22,23]. Therefore, to use Ca addition for the desulfurization process or the prevention of S segregation at the interface of oxides and substrate, it is important to find the balance between the amount of Ca and S within the melt and understand the order of the reaction that is likely to occur. On the other hand, using stable oxides such as CaO in the beginning will lead to the reduction process since, according to the calculations in equations (6-8), it is thermodynamically beneficial to form calcium aluminates. This likely requires the formation of Al_2O_3 beforehand, which can be achieved by the reduction of CaO [12-16]. The formation of Ca from this process will most likely initiate the formation of sulfides. This process is presumably the same for Ni-base superalloys as well.

V. Conclusion

To conclude, the following has been made clear about the effect of Ca addition on the oxidation resistance of Ni-Al single crystal alloy.

1. Ca addition succeeded in the desulfurizing of the alloy and the forming of CaS. By increasing the amount of Ca, the amount of S that has been removed and the CaS that had formed increased as well. But with the increase in Ca addition, parts of the slags that had formed were involved within the melt, negatively affecting the oxidation resistance of the sample. The usage of filters may help solve this problem.
2. Ca addition of 20 ppm improved the oxidation resistance of the alloy, compared to Ni-Al (0 ppm Ca). But it has not improved as much as the sample melted in the CaO crucible. This is likely due to the amount and the order of the reaction of Ca that had reacted to desulfurize and prevent the segregation of S by the formation of CaS. Increasing the amount of Ca addition increased the amount of desulfurization and formation of CaS, but slag formation had also increased as well.
3. The dominating reaction for Ca addition was the formation of oxides. In order to efficiently desulfurize, form CaS, and prevent the negative effect of Ca on the oxidation resistance, the formation of sulfides has to be the dominating reaction. Using CaO will help by initiating the reduction of CaO to produce Ca, which will react with the S within the melt.

Acknowledgments

This research was financially supported by the Council for Science, Technology and Innovation (CSTI), Cross-ministerial Strategic Innovation Program (SIP), “Materials Integration for revolutionary design system of structural materials” (Funding agency: JST). The authors would like to express our gratitude to Dr. Makoto Osawa for the helpful discussions. We also would like to thank Ms. Kyoko Suzuki for the support of microstructural investigation, and Mr. Yuji Takata for the preparation of the single crystal alloys.

Conflict of Interest

On behalf of all authors, the corresponding author states that there is no conflict of interest.

References

[1] K. Harris, G.L. Erickson, S.L. Sikkenga, W.D. Brentnall, J.M. Aurrecoechea, and K.G. Kubarych: *Superalloys 1992*, 1992, pp. 297-306.

[2] A.W. Fundenbusch, J.G. Smeggil, and N.S. Bornstein: *Metall. Mater. Trans. A*, 1985, vol. 16A, pp. 1164-66.

[3] Y. Ikeda, M. Tosa, K. Yoshihara, and K. Nii: ISIJ International, 1989, vol. 29, pp. 966-72.

[4] M. A. Smith, W. E. Frazier, and B. A. Pregger: *Mat. Sci. Eng. A*, 1995, vol. 203, pp. 388-98.

[5] J. L. Smialek, and B. A. Pint: *Mat. Sci. Forum*, 2001, vols. 369-372, pp. 459-66.

[6] N. Birks, G.H. Meier, and F.S. Pettit: *Introduction to the High-Temperature Oxidation of Metals*, 2nd ed., Cambridge University Press, New York, 2006, pp.144-48.

[7] E. Fedorova, D. Monceau, and D. Oquab: *Corr. Sci.*, 2010, vol. 52, pp. 3932-42.

[8] J. Smialek: *Crystal*, 2021, vol. 11, pp. 60-71.

[9] J. L. Smialek, Oxid. Met., 2022, vol. 97, pp. 1-50.

[10] H. Harada, K. Kawagishi, T. Kobayashi, T. Yokokawa, M. Osawa, M. Yuyama, S. Suzuki, Y. Joh, and S. Utada: US Patent, patent number 10689741 (2020.06.23)

[11] S. Utada, Y. Joh, M. Osawa, T. Yokokawa, T. Kobayashi, K. Kawagishi, S. Suzuki, and H. Harada: *Superalloys 2016*, 2016, pp. 591-9.

[12] S. Utada, Y. Joh, M. Osawa, T. Yokokawa, T. Sugiyama, T. Kobayashi, K. Kawagishi, S. Suzuki, and H. Harada: *Met. Mat. Trans. A.*, 2018, vol. 49A, pp. 4029-41.

[13] T. Sugiyama, S. Utada, T. Yokokawa, M. Osawa, K. Kawagishi, S. Suzuki, and H. Harada: *Met. Mat. Trans. A.*, 2019, vol. 50, pp. 3903-11.

[14] C. Tabata, K. Kawagishi, J. Uzuhashi, T. Ohkubo, K. Hono, T. Yokokawa, H. Harada, and S. Suzuki: *Scr. Mater.*, 2021, vol. 194, 113616.

[15] Y. Kishimoto, T. Kono, T. Horie, T. Yokokawa, M. Osawa, K. Kawagishi, S. Suzuki, and H. Harada: *Met. Mat. Trans. B.*, 2021, vol. 52B, pp. 1450-62.

[16] C. Tabata, K. Kawagishi, J. Uzuhashi, T. Ohkubo, T. Yokokawa, H. Harada, S. Suzuki: *Met. Mat. Trans. A.*, 2022, vol. 53, pp. 2452-8.

[17] T. Yokokawa, H. Harada, K. Kawagishi, M. Sakamoto, M. Osawa, Y. Takata, M. Yuyama, T. Kobayashi, T. Sugiyama, and S. Suzuki: *Superalloys 2020*, TMS, Seven Springs, Champion, PA, 2020, pp. 400-7.
[18] T. Xu, Y. Su, T. Shi, and X. Zhang: *Ceram. Int.*, 2021, vol. 47, pp. 2165-71.
[19] M. Chen, N. Wang, J. Yu, and A. Yamaguchi: *J. Eur. Ceram. Soc.*, 2007, vol. 27, pp. 1953-9.
[20] Y. Azakli, K. O. Gunduz, S. Cengiz, Y. Gencer, and M. Tarakci: *Oxid. Met.*, 2021, vol. 95, pp. 135-56.
[21] J. J. deBarbadillo: *Superalloys 1976*, Seven Springs, Champion, PA, 1976, pp. 95-107.
[22] T. Gheno, G. H. Meier, and B. Gleeson: *Oxid. Met.*, 2015, vol. 84, pp. 185-209.
[23] K. T. Chiang, G. H. Meier, and R. A. Perkins: *J. Mater. Energ. Syst.*, 1984, vol. 6, pp. 71-86.
[24] K. Jung, F. S. Pettit, and G. H. Meier, *Mater. Sci. Forum*, 2008, vol. 595-598, pp. 805-12.
[25] R. J. Fruehan: *Metall. Trans. B*, 1978, vol. 9B, pp. 287-92.
[26] T. Degawa and T. Ototani: *Tetsu-to-Hagané*, 1987, vol. 73, pp. 1684-90.
[27] J. F. Elliot and M. Gleiser: *Thermochemistry for Steelmaking*, vol. 1, Addison-Wesley, 1960.
[28] S. Nagasaki: *Metals Databook 3rd edition*, Japan Institute of Metals and Materials, Japan, 1993, pp. 96-7.
[29] I. Barin: *Thermochemical Data of Pure Substances*, 3rd ed., VCH Verlagsgesellschaft mbH, Weinheim and VCH Publishers, Inc., New York, NY, 1995.